Pergamon

Int. J. Solids Structures Vol. 34, No. 30, pp. 3941–3951, 1997

0020-7683/97 $17.00 + .00

PII: S0020-7683(97)00018-8

A MODEL OF EVOLVING DAMAGE BANDS IN MATERIALS

Y. HUANG
Department of Mechanical Engineering—Engineering Mechanics,
Michigan Technological University, Houghton, MI 49931, U.S.A.

X. Y. GONG and Z. SUO
Department of Mechanical and Environmental Engineering, University of California,
Santa Barbara, CA 93106, U.S.A.

and

Z. Q. JIANG
Department of Mechanical Engineering—Engineering Mechanics,
Michigan Technological University, Houghton, MI 49931, U.S.A.

(*Received* 31 *March* 1996; *in revised form* 9 *December* 1996)

Abstract—This paper develops a model that incorporates damage band evolution at three levels: (i) at the mechanism level, the damage mechanisms, such as diffusive void growth and fatigue cracks, determine the damage growth rate; (ii) at an intermediate level, the damage band is modeled as springs connecting undamaged materials, and the spring constants change as damage develops; (iii) at the continuum level, the damage band is modeled as an array of dislocations to satisfy equilibrium. We demonstrate this model with an example of a band of microcracks subject to remote tensile cyclic stress. It is observed that damage rapidly grows at the weakest regions in the band, and a macroscopic crack nucleates while the overall damage level is still very low. The model shows that there exists a critical number of cycles for macroscopic crack nucleation, $N_{\text{nucleation}}$, which depends on materials as well as the amplitude of applied cyclic stress. This critical number of cycles is insensitive to the size of damage cluster, but decreases rapidly as the local excess of damage increases. © 1997 Elsevier Science Ltd.

1. INTRODUCTION

Engineering materials exhibit time-dependent degradation and failure under creep, stress-corrosive cracking, or cyclic loading conditions. Although failure mechanisms vary in different materials, they all display one common characteristic: damage originates from localized regions and evolves to a macroscopic crack. The present paper investigates the evolution of localized damage bands over time/cycles, and the relation between micro-damage and macroscopic nucleation of defects. Following an earlier attempt (Ye, 1992), the model includes three levels—the mechanism level, the intermediate level, and the continuum level. (i) At a sufficiently fine resolution, damage processes such as power law creep voids, diffusive voids, shear fatigue cracks are incorporated to determine the damage growth rate. (ii) At an intermediate level, localized damage bands are modeled as springs connecting undamaged materials. The spring compliances are nonuniform, increasing as the damage evolves. (iii) At the continuum level, the localized damage band, growing in an otherwise undamaged material, is modeled as an array of dislocations. The equilibrium provides the governing equation for the local stress. The model estimates the critical time or cycle number at which a macroscopic defect nucleates. For simplicity, the model is limited to two dimensional analysis.

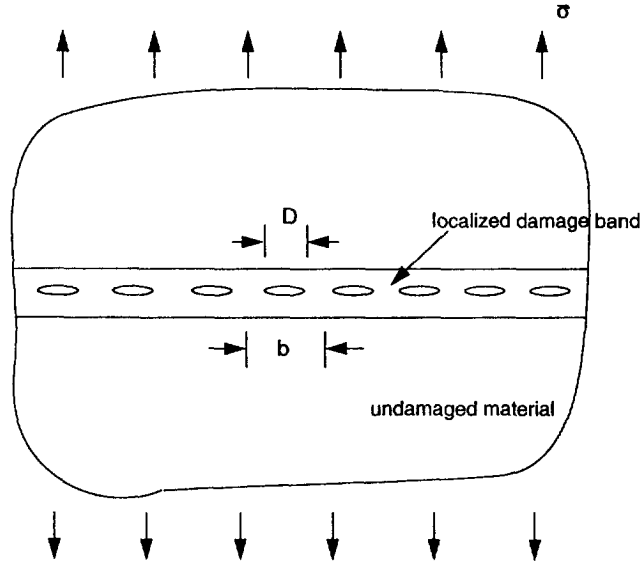

Fig. 1. A localized damage band, where b is the average spacing between microscale damage, and D is the average size of microscale damage.

2. GENERAL DESCRIPTION OF THE MODEL

Figure 1 shows an example of damage band. It is a weak region in an otherwise elastic material, and is the potential band for deformation localization. The thickness of the band is much smaller than the characteristic length of the sample. The material is assumed to be subject to remote uniform tensile stress $\bar{\sigma}$. Other types of loading can be analyzed similarly, such as shear fatigue (Ye, 1992) and thermal cycling (Huang *et al.*, 1997). Three levels discussed in the previous section are prescribed in the following.

2.1. *Mechanism level*

Let ω be the nondimensional damage parameter, such as the normalized microcrack size or void size. The limit $\omega = 0$ corresponds to the undamaged state in the material. Its growth rate, in general, is governed by the current damage state and the local stress σ, i.e.,

$$\frac{\partial \omega}{\partial t} = \frac{1}{t_0}\bar{F}\left(\frac{\sigma}{\sigma_0}, \omega\right) \tag{1}$$

where t is the time or cycle number, t_0 is a reference time or cycle number, σ_0 is a reference stress, and function $\bar{F}$ depends on the specific damage mechanism in the material. For many damage mechanisms, the damage evolution rate can be related to the local stress σ through a power law

$$\frac{\partial \omega}{\partial t} = \frac{1}{t_0}F(\omega)\left(\frac{\sigma}{\sigma_0}\right)^n \tag{2}$$

where the power n is a material property, and the nondimensional function $F(\omega)$ represents the damage growth rate when the local stress reaches the reference stress. In general, $F(\omega)$ is a monotonically increasing function of ω since the damage growth rate increases with the damage level.

2.2. *Intermediate level*

Beyond the elastic stretch in the undamaged material, there is an additional stretch across the band, δ, due to localized damage. The additional stretch δ is related to the local stress σ through a bridging law,

$$\frac{\delta}{\delta_0} = \bar{C}\left(\frac{\sigma}{\sigma_0}, \omega\right) \tag{3}$$

where δ_0 is a material length, and the function $\bar{C}$ can be obtained from a micromechanics model for the specific damage mechanism in the material. In cases such as in stress corrosion cracking (Cao *et al.*, 1987) or shear fatigue (Ye, 1992), the stretch is linear in the stress so that eqn (3) can be written as

$$\frac{\delta}{\delta_0} = C(\omega)\frac{\sigma}{\sigma_0} \tag{4}$$

where $C(\omega)$ is the linear spring compliance, which is also a monotonically increasing function of ω since the spring is more compliant as the damage level increases.

2.3. *Continuum level*

The localization band can be regarded as an array of dislocations. The local stress in the band, σ, is caused by the remote uniform stress, $\bar{\sigma}$, and by the dislocations (Rice, 1968):

$$\sigma(x) = \bar{\sigma} - \frac{E'}{4\pi}\int_{-\infty}^{\infty} \frac{\partial\delta(\xi)}{\partial\xi}\frac{\mathrm{d}\xi}{x-\xi} \tag{5}$$

where E' is Young's modulus E for plane stress or $E/(1-\nu^2)$ for plane strain, ν is Poisson's ratio, and x is the coordinate in the direction of the band.

The distribution of the damage state ω, the additional stretch δ, and the local stress σ are governed by the differential and integral equations in eqns (2), (4) and (5). For a given initial damage distribution, these governing equations can be solved numerically to evolve the damage distribution as time or cycle increases.

3. MICROCRACK DAMAGE IN FATIGUE AND THE NUCLEATION OF A MACROSCOPIC CRACK

The model outlined in the previous section is demonstrated here through an example of microcracks in a localized band subjected to remote tensile cyclic stress, $\Delta\bar{\sigma}$. As shown in Fig. 1, the average spacing between microcracks is b, and the average size of microcracks is D. The damage parameter ω is defined by

$$\omega = \frac{D}{b}. \tag{6}$$

The limit $\omega = 0$ corresponds to an undamaged material, while $\omega = 1$ represents the critical state when microcracks coalesce and a macroscopic crack nucleates.

3.1. *Mechanism level: damage evolution rate*

The damage mechanism in this example is the fatigue growth of microcracks. There have been extensive studies on small fatigue cracks (e.g., Suresh and Ritchie, 1984, also Suresh, 1991, for detailed discussion and documentation). The fatigue growth rate of microcracks is influenced by many factors, such as microstructures (e.g., Pearson, 1975, Lankford, 1982, Tanaka *et al.*, 1983), T-stress level, plastic zone size, crack closure effect around tips of microcracks (e.g., Allen and Sinclair, 1982, Suresh and Ritchie, 1984, Fleck and Newmann, 1988), and environmental effect (e.g., Gangloff, 1981). Dowling (1977) suggested that the cyclic J-integral ΔJ provides a measure of the driving force for fatigue growth of small cracks, and the growth rate is approximately proportional to ΔJ^m (m is a material property). Though the following analysis can be applied to any laws governing fatigue growth of microcracks, Paris law is used here for simplicity,

$$\frac{\mathrm{d}D}{\mathrm{d}N} = \beta(\Delta K)^n \tag{7}$$

where N is the number of cycles, β and n are material properties, and ΔK is the cyclic stress intensity factor at a microcrack tip. For the configuration in Fig. 1, ΔK is related to the cyclic local stress $\Delta\sigma$ by (see Appendix A for details)

$$\Delta K = \Delta\sigma\sqrt{b\tan\frac{\pi}{2}\omega} \tag{8}$$

where b is the average spacing between microcracks in the band. The damage growth rate can then be found as

$$\frac{\mathrm{d}\omega}{\mathrm{d}N} = \beta b^{n/2-1}\sigma_0^n F(\omega)\left(\frac{\Delta\sigma}{\sigma_0}\right)^n \tag{9}$$

where

$$F(\omega) = \left(\tan\frac{\pi}{2}\omega\right)^{n/2}. \tag{10}$$

3.2. *Intermediate level: bridging law*

Due to the presence of microcracks, there is an additional cyclic stretch across the band, $\Delta\delta$, beyond the uniform stretch associated with undamaged materials. This additional cyclic stretch comes from the cyclic opening of microcracks in the band. A micromechanics model is described in Appendix A, and $\Delta\delta$ is related to the cyclic local stress $\Delta\sigma$ by the bridging law

$$\Delta\delta = \frac{4}{\pi}\frac{b}{E'}\ln\frac{1}{\cos\left(\frac{\pi}{2}\omega\right)}.\Delta\sigma. \tag{11}$$

It can be rewritten as

$$\frac{\Delta\delta}{b\frac{\sigma_0}{E'}} = C(\omega)\frac{\Delta\sigma}{\sigma_0} \tag{12}$$

where

$$C(\omega) = \frac{4}{\pi}\ln\frac{1}{\cos\left(\frac{\pi}{2}\omega\right)}. \tag{13}$$

For an undamaged material ($\omega = 0$), $C(\omega)$ is zero such that there is no additional cyclic stretch. In the other limit when microcracks start to coalesce ($\omega = 1$), $C(\omega)$ approaches to infinity so that the local stress is zero and the spring is completely broken. Therefore, there is no bridging at this moment ($\omega = 1$) and a macroscopic crack is nucleated.

3.3. *Continuum level: stress equilibrium*

For a uniform remote cyclic stress $\Delta\bar{\sigma}$, the stress equilibrium eqn (5) takes the form

$$\Delta\sigma(x) = \Delta\bar{\sigma} - \frac{E'}{4\pi}\int_{-\infty}^{\infty} \frac{\partial\Delta\delta(\xi)}{\partial\xi}\cdot\frac{\mathrm{d}\xi}{x-\xi}. \tag{14}$$

For a given damage distribution $\omega(x)$, eqns (12) and (14) give a linear integral equation for $\Delta\sigma$ (or $\Delta\delta$).

3.4. *Normalization*

An important equivalence between the amplitude of applied cyclic stress $\Delta\bar{\sigma}$ and number of cycles N can be established by the following normalization:

$$N' = \frac{N}{\beta^{-1}b^{1-(n/2)}(\Delta\bar{\sigma})^{-n}}, \sigma' = \frac{\Delta\sigma}{\Delta\bar{\sigma}}, \delta' = \frac{\Delta\delta}{b\dfrac{\Delta\bar{\sigma}}{E'}}, x' = \frac{x}{b}. \tag{15}$$

The governing eqns (9), (12) and (14) then become

$$\frac{\partial\omega}{\partial N'} = F(\omega)(\sigma')^n \tag{16a}$$

$$\delta' = C(\omega)\sigma' \tag{16b))}$$

$$\sigma' = 1 - \frac{1}{4\pi}\int_{-\infty}^{\infty} \frac{\partial\delta'}{\partial\xi'}\cdot\frac{\mathrm{d}\xi'}{x'-\xi'}. \tag{16c}$$

It is evident that the number of cycles N appears together with the amplitude of remote cyclic stress $(\Delta\bar{\sigma})^n$ through the normalized cycle number N'. Therefore, a small amplitude of applied cyclic stress $\Delta\bar{\sigma}$ is equivalent to a large number of cycles, and vice versa. This is similar to the S-N curve in the empirical fatigue design. (This conclusion results from the Paris law, and may not hold for non-power law damage growth rate.)

At a given cycle N', the damage distribution $\omega(x')$ is known. The combination of eqns (16b) and (16c) solve the stress distribution $\sigma'(x')$, and then eqn (16a) updates the damage distribution $\omega(x')$ for an increment of cycle $\Delta N'$. The procedure then repeats for the next cycle number, $N'+\Delta N'$.

3.5. *Initial distribution of damage in the band*

The damage parameter ω is considered as a continuum variable in the continuum analysis. This is rather similar to the Gurson's (1975) model for a voided, dilating material, which was derived from a cell analysis, but has been successfully applied in the continuum theory. Following Ohno and Hutchinson (1984) and Huang and Hutchinson (1989), the following initial damage distribution is taken to represent a cluster of damage in the band

$$\omega(x) = \omega_{\text{average}} + (\omega_{\max} - \omega_{\text{average}})\exp\left[-\frac{1}{2}\left(\frac{x}{\lambda b}\right)^2\right] \tag{17}$$

where ω_{average} and $\omega_{\max}$ are the average and maximum damage level in the band, and $2\lambda b$ represents the size of the damage cluster. The nondimensional parameter $\omega_{\max}-\omega_{\text{average}}$ and 2λ characterize the excess of damage in the band and ratio of the size of damage cluster to average microcrack spacing, respectively.

3.6. *Results and discussions*

Details of the numerical method to solve governing eqn (16) are given in Appendix B. A value of power $n = 2$ is fixed in the present study. Results in Figs 2–4 are for initial damage parameters $\omega_{\text{average}} = 0.01$, $\omega_{\max} = 0.10$, and $2\lambda = 1$. This represents a highly localized cluster of damage that has the size of approximately b, and the excess of damage in the band is much larger than the average damage level. The initial damage profile is shown in Fig. 2, vs the normalized distance in the band, x/b. As the cycle number increases, the damage distribution evolves very nonuniformly in the band. Damage at the center ($x = 0$) increases significantly faster than the average level (Fig. 2). For example, ω increases from 0.1 to 1 at the center while the average ω is changed by approximately 0.1. Therefore, damage evolution is rather concentrated at the weakest regions in the material. This is similar to the deformation localization in voided ductile materials (Ohno and Hutchinson, 1984, Huang and Hutchinson, 1989).

The distributions of additional stretch δ and local stress σ are shown in Figs 3 and 4, respectively. It is observed that the evolutions of δ and σ are also very concentrated. As the damage parameter ω at the center approaches one, the corresponding additional stretch is much larger than the average level, and the local stress approaches zero such that bridging effect starts to disappear at the center. The number of cycles at this moment is critical because microcracks start to coalesce and a macroscopic crack is to be nucleated. This critical number of cycles for crack nucleation, denoted by $N_{\text{nucleation}}$, characterizes the maximum number of cycles the material can sustain before a macroscopic crack appears. It depends on the material, the amplitude of applied cyclic stress $\Delta\bar{\sigma}$, as well as the initial distribution of damage in the band. For initial damage parameters given above, this critical number is $N_{\text{nucleation}} = 1.503\beta^{-1}b^{1-(n/2)}(\Delta\bar{\sigma})^{-n}$ (Fig. 2).

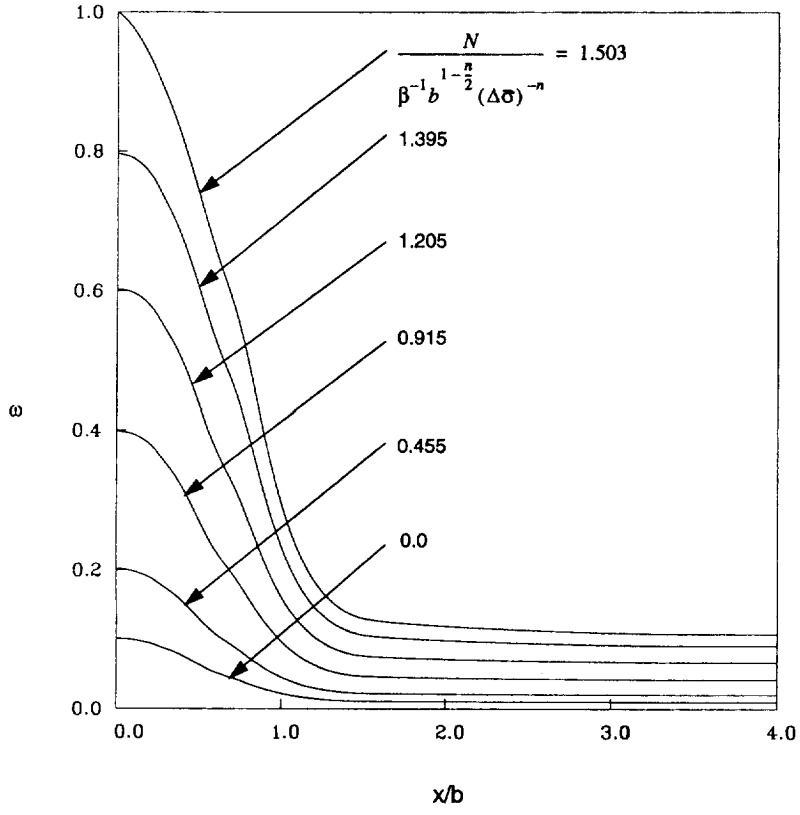

Fig. 2. Damage distribution, ω, in the band for several normalized number of cycles, $\beta b^{(n/2)-1}(\Delta\bar{\sigma})^n N$, where the average initial damage level $\omega_{\text{average}} = 0.01$, excess of damage in the band $\omega_{\max} - \omega_{\text{average}} = 0.09$, normalized size of the damage cluster $2\lambda = 1$, power $n = 2$, and b is the average spacing between microcracks. The number of cycles when ω reaches one is the critical number cycle for crack nucleation, $N_{\text{nucleation}}$.

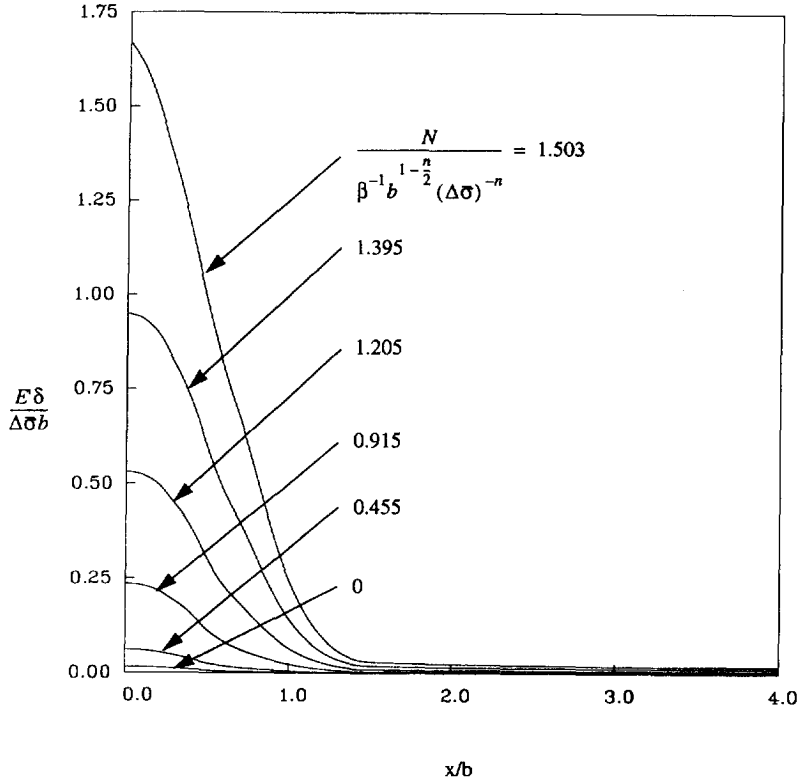

Fig. 3. The distribution of normalized additional stretch across the band for several number of cycles, $\beta b^{(n/2)-1}(\Delta\bar{\sigma})^n N$, where the average initial damage level $\omega_{\text{average}} = 0.01$, excess of damage in the band $\omega_{\max} - \omega_{\text{average}} = 0.09$, normalized size of the damage cluster $2\lambda = 1$, power $n = 2$, and b is the average spacing between microcracks.

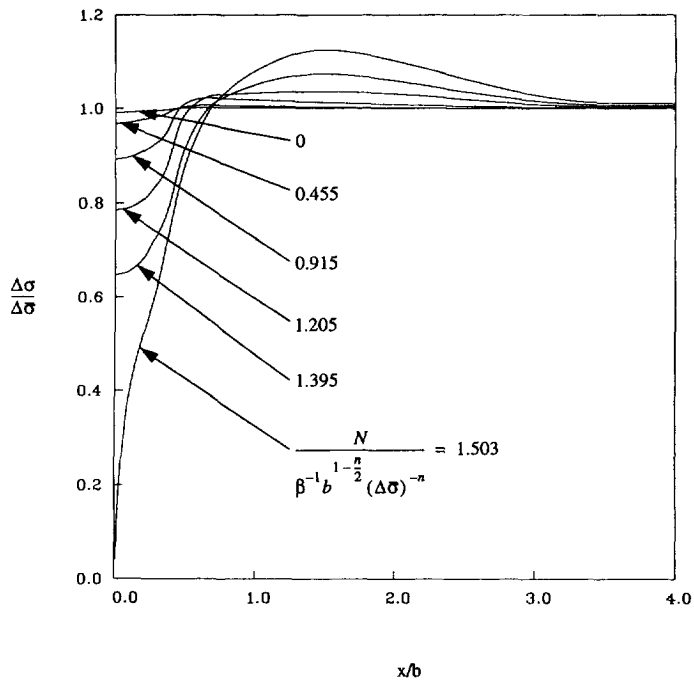

Fig. 4. The distribution of normalized stress in the band for several number of cycles, $\beta b^{(n/2)-1}(\Delta\bar{\sigma})^n N$, where the average initial damage level $\omega_{\text{average}} = 0.01$, excess of damage in the band $\omega_{\max} - \omega_{\text{average}} = 0.09$, normalized size of the damage cluster $2\lambda = 1$, power $n = 2$, and b is the average spacing between microcracks.

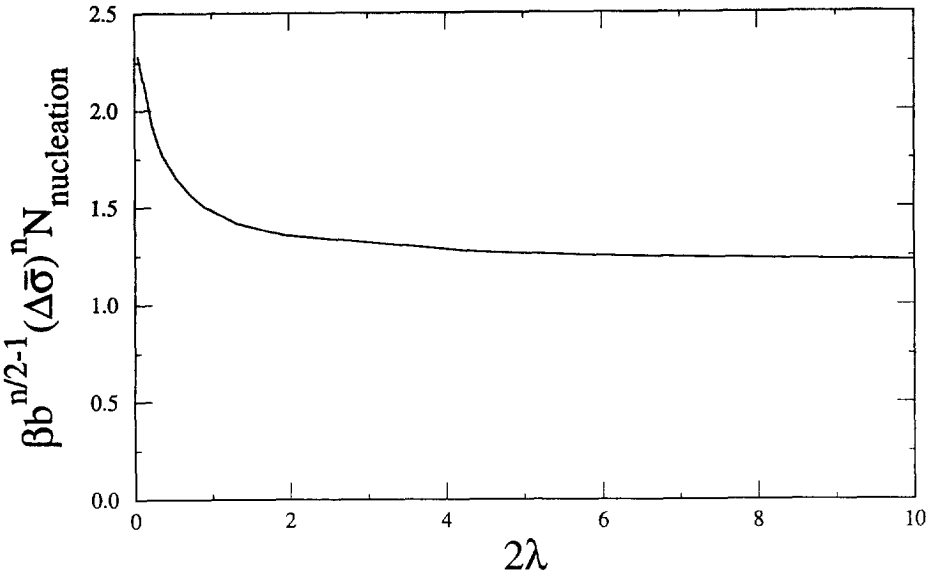

Fig. 5. The normalized critical number of cycles for crack nucleation, $\beta b^{(n/2)-1}(\Delta\bar{\sigma})^n N_{\text{nucleation}}$, vs the normalized size of damage cluster, 2λ, for the average initial damage level $\omega_{\text{average}} = 0.01$, excess of damage in the band $\omega_{\max} - \omega_{\text{average}} = 0.09$, and power $n = 2$.

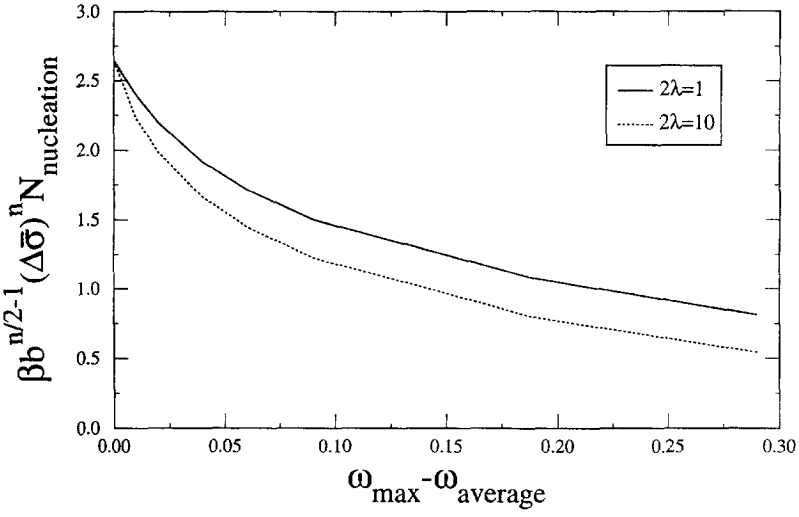

Fig. 6. The normalized critical number of cycles for crack nucleation, $\beta b^{(n/2)-1}(\Delta\bar{\sigma})^n N_{\text{nucleation}}$, vs the excess of damage in the band, $\omega_{\max} - \omega_{\text{average}}$, for a small damage cluster ($2\lambda = 1$) as well as a large one ($2\lambda = 10$), where the average initial damage level $\omega_{\text{average}} = 0.01$, and power $n = 2$.

The normalized critical number of cycles for crack nucleation, $\beta b^{(n/2)-1}(\Delta\sigma)^n N_{\text{nucleation}}$, is shown in Fig. 5 vs the normalized cluster size 2λ for $\omega_{\max} = 0.10$, $\omega_{\text{average}} = 0.01$ and power $n = 2$. As the cluster size increases, the critical number of cycles rapidly approaches to an asymptote, approximately $1.2\beta^{-1} b^{1-n/2}(\Delta\bar{\sigma})^{-n}$. Therefore, only small damage clusters whose sizes are less than twice the microcrack spacing can achieve a significant increase in the critical numbers of cycles (Fig. 5), hence to improve the fatigue life of the material.

The normalized critical number of cycles for crack nucleation, $\beta b^{(n/2)-1}(\Delta\bar{\sigma})^n N_{\text{nucleation}}$, is shown in Fig. 6,, vs the excess damage in the band, $\omega_{\max} - \omega_{\text{average}}$, for a small cluster ($2\lambda = 1$) as well as a large one ($2\lambda = 10$). It is clearly observed that the critical number of cycles for crack nucleation is rather insensitive to the size of the damage cluster since two curves in Fig. 6 are very close. However, the critical number of cycles is reduced significantly as the excess of damage in the band increases. One can conclude that the nucleation of a

macroscopic crack is very sensitive to the local excess of damage, but not the size of a damage cluster.

4. CONCLUDING REMARKS

A model is presented to investigate damage evolution in a localized weak zone in materials. It includes modeling at three different levels: (i) on the mechanism level, damage mechanisms, such as diffusive void growth, fatigue cracks, are incorporated to determine the damage growth rate; (ii) on an intermediate level, localized damage bands are modeled as springs connecting undamaged materials, and spring constants are obtained from micromechanics models; (iii) on the continuum level, a localized damage band is modeled as an array of dislocations governed by the stress equilibrium.

The model is demonstrated through an example of microcracks in a localized band subjected to remote tensile cyclic stress. It is observed that damage evolution is rather concentrated at the weakest regions in the material, where damage rapidly accumulates and a macroscopic crack nucleates while the overall damage level is still very low. The model shows that there exists a critical number of cycles for crack nucleation, $N_{\text{nucleation}}$, which depends on the material, the amplitude of applied cyclic stress, as well as the initial distribution of damage in the band. This critical number of cycles for crack nucleation is found to be relatively insensitive to the size of a damage cluster, but decreases rapidly as the local excess of damage increases.

The assumptions made in the above demonstrational example significantly simplify the analysis without changing the time-dependent degradation characteristics in materials. They can be improved by incorporating realistic material features in the model. For example, the cluster of defects in eqn (17) can be replaced by realistic nonuniform defect distributions in materials (Boucier *et al.*, 1986, Spitzig *et al.*, 1988, Huang, 1993). The material and component geometries under complex loading conditions can be studied by the finite element method on the continuum level instead of the integral equation approach in eqn (5). The evolution of some damage (such as fatigue growth of microcracks, see Suresh, 1991) follows eqn (1) rather than the power law in eqn (2). The nonlinear bridging law in eqn (3) may be more appropriate than the linear one in eqn (4) for certain materials and loadings. By incorporating all these features in the analysis, the present model has the potential to connect the damage evolution process on the mechanism level to the material and component design on the continuum level.

Acknowledgements - YH gratefully acknowledges the financial support from NSF Grant No. INT-94-23964 and from the ALCOA Foundation. The work done at UCSB was supported by ARPA through a URI contract N-0014-92-J-1808.

REFERENCES

Allen, R. J. and Sinclair, J. C. (1982) The behavior of short cracks. *Fatigue Engineering Materials Structures* **5**, 343–347.

Boucier, R. J., Koss, D. A., Smelser, R. E. and Richmond, O. (1986) The influence of porosity on the deformation and fracture of alloys. *Acta Metallica Materiala* **34**, 2443.

Cao, H. C., Dalgleish, B. J., Hsueh, C. H. and Evans, A. G. (1987) High-temperature stress corrosion cracking in ceramics. *Journal of the American Ceramic Society* **70**, 257–264.

Dowling, N. E. (1977) Crack growth during low-cycle fatigue of smooth axial specimens. In *Cyclic Stress-Strain and Plastic Deformation Aspects of Fatigue Crack Growth*, STP 637, pp. 97–121. American Society of Testing and Materials, Philadelphia.

Fleck, N. A. and Newmann, J. C. (1988) Analysis of crack closure under plane strain conditions. In *Mechanics of Fatigue Crack Closure*, STP 982, pp. 319–341. American Society of Testing and Materials, Philadelphia.

Gangloff, R. P. (1981) The criticality of crack size aqueous corrosion fatigue. *Research Mechanica Letters* **1**, 299–306.

Gurson, A. L. (1975) Plastic flow and fracture behavior of ductile materials incorporating void nucleation, growth and interaction. Ph.D. thesis, Brown University.

Huang, Y. (1993) The role of nonuniform particle distribution in plastic flow localization. *Mechanics of Materials* **16**, 265.

Huang, Y. and Hutchinson, J. W. (1989) A model study of the role of nonuniform defect distribution on plastic shear localization. In *Role of Modeling in Materials Design*, ed. Embury, J. D., AIME, p. 129.

Huang, Y., Jiang, Z. Q., Chandra, A., Hu, K. X. and Yeh, C.-P. (1997) A model study of thermal fatigue in layered electronic assemblies. *ASME Transactions.—Journal of Electronic Packaging* (submitted).
Lankford, J. (1982) The growth of small fatigue cracks in 7075-T6 aluminium. *Fatigue Engineering Materials Structures* **5**, 233–248.
Ohno, N. and Hutchinson, J. W. (1984) Plastic flow localization due to non-uniform void distribution. *Journal of the Mechanics and Physics of Solids* **32**, 63–85.
Pearson, S. (1975) Initiation of fatigue cracks in commercial aluminum alloys and the subsequent propagation of very short cracks. *Engineering Fracture Mechanics* **7**, 235–247.
Rice, J. R. (1968) Mathematical analysis in the mechanics of fracture. In *Fracture: An Advanced Treatise*, ed. Liebowitz, H. vol. 2. Academic Press, New York, pp. 191–311.
Spitzig, W. A., Smelser, R. E. and Richmond, O. (1988) The evolution of damage and fracture in iron compacts with various initial porosities. *Acta Metallica Materiala* **36**, 1201.
Suresh, S. (1991) *Fatigue of Materials*. Cambridge University Press, Cambridge, England.
Suresh, S. and Ritchie, R. O. (1984) Propagation of short fatigue cracks. *International Metals Reviews* **29**, 445–476.
Tada, H., Paris, P. C. and Irwin, G. R. (1985) *The Stress Analysis of Cracks Handbook*. Del. Research, St. Louis, MO.
Tanaka, K., Hojo, M. and Nakai, Y. (1983) Crack initiation and early propagation in 3% silicon iron. In *Fatigue Mechanisms: Advances in Quantitative Measurement of Fatigue Damage*, STP 811, pp. 207–232. American Society of Testing and Materials, Philadelphia.
Ye, T. (1992) The Micromechanics of Shear Fatigue. MS thesis, Dept. Mech. Engr., Univ. California, Santa Barbara.

APPENDIX A

The additional stretch across the band, δ, comes from the opening of microcracks. By averaging the crack opening displacement in the band (Fig. 1), one has

$$\delta = \frac{1}{b}\int_{-D/2}^{D/2} \delta_{\text{open}}\,\mathrm{d}x \tag{A1}$$

where δ_{open} is the crack opening displacement, and can be estimated using a configuration of periodically distributed cracks as (Tada *et al.*, 1985)

$$\delta_{\text{open}} = \frac{4\sigma b}{\pi E'}\cos h^{-1}\frac{\cos\dfrac{\pi x}{b}}{\cos\dfrac{\pi D}{2b}} \quad \text{for } |x| \leqslant \frac{D}{2}. \tag{A2}$$

The substitution of eqn (A2) into eqn (A1) leads to eqn (11).

For periodically distributed microcracks in Fig. 1, the stress intensity factor is (Tada *et al.*, 1985)

$$K = \sigma\sqrt{b\tan\frac{\pi D}{2b}} \tag{A3}$$

which becomes the same as eqn (8) by changing K and σ to ΔK and $\Delta\sigma$, respectively.

APPENDIX B

From symmetry $\sigma(-x) = \sigma(x)$ and $\delta(-x) = \delta(x)$, eqns (16b) and (16c) can be rearranged to

$$\frac{\delta(x)}{C(\omega)} = 1 - \frac{1}{2\pi}\int_0^x \frac{\xi}{x^2 - \xi^2}\frac{\partial\delta}{\partial\xi}\mathrm{d}\xi \quad \text{for } x > 0. \tag{B1}$$

By the following change of variables, the interval $(0, +\infty)$ for x and ξ is transformed to $(-1, 1)$ for u and t

$$x = \frac{1+u}{1-u}, \xi = \frac{1+t}{1-t}. \tag{B2}$$

For each given damage profile $\omega(x)$, the additional stretch δ is expanded in terms of Chebyshev polynomial

$$\delta(u) = \sum_{j=1}^{M} a_j T_{j-1}(u) \tag{B3}$$

where T_j is the Chebyshev polynomial of degree j, and a_j is the coefficient to be determined. By the standard collocation method, eqn (B1) becomes M linear algebraic equations and can be solved numerically.

Equation (16a) is an ordinary differential equation for the damage parameter ω. It can be solved by the Runge-Kutta method if the local stress distribution $\sigma(x)$ is known. Therefore, the numerical procedures to obtain the damage state ω, local stress σ, and additional stretch δ are

I. For the initial damage distribution $\omega(x)$ in eqn (17), solve the integral eqn (B1) by the expansion [eqn (B3)] and collocation method in order to obtain the distribution of the additional stretch $\delta(x)$ and local stress $\sigma(x)$ in the band;

III. For the known local stress distribution $\sigma(x)$, solve eqn (16a) by the Runge-Kutta method and get the new damage distribution $\omega(x)$ at the next cycle;

III. For the new damage distribution $\omega(x)$, solve eqn (B1) in order to get the corresponding additional stretch $\delta(x)$ and local stress $\sigma(x)$ for this cycle;

IV. Repeat steps II and III until the maximum value of ω in the band reaches 1. The corresponding number of cycles is the critical cycle number for crack nucleation.